Comparative Crashworthiness Assessment of the ULSAB-AVC model with Advance High Strength Steel and Conventional Steel

Johnheon Yoon[1] · Hoon Huh[1] · Seho Kim[2] · Hongkee Kim[3] · Seungho Park[3]

[1] Department of Mechanical Engineering, Korea Advanced Institute of Science and Technology, Science town, Daejeon, 305-701, Korea

[2] School of Automotive, Industrial and Mechanical Engineering, Daegu University, 15 Naeri, Jillyang, Gyeongsan, Gyeonbuk, 712-714, Korea

[3] POSCO Technical Research Laboratories, 699, Cumho-dong, Gwangyang, Jeonnam, 545-090, Korea

Abstract

As the regulation and assessment program for passenger safety become stringent, automakers are required to develop light and safe vehicles. In order to fulfill both requirements which conflict with each other, automobile and steel companies have proposed the application of AHSS(Advance High Strength Steel) such as DP, TRIP and martensite steel. ULSAB-AVC model is one of the most remarkable reactions to offer solutions with the use of steel for the challenge to simultaneously improve the fuel efficiency, passenger safety, vehicle performance and affordability. This paper is concerned with the crash analysis of ULSAB-AVC model according to the US-SINCAP in order to compare the effectiveness between the model with AHSS and that with conventional steels. The crashworthiness is investigated by comparing the deformed shape of the cabin room, the energy absorption characteristics and the intrusion velocity of a car.

Keywords: Crashworthiness, Side impact analysis, ULSAB-AVC(Ultra Light Steel Auto Body Advanced Vehicle Concepts), AHSS(Advance High Strength Steel), US-SINCAP(U. S. Side Impact test for New Car Assessment Program)

1. Introduction

Light-weight design of an auto-body is a challenging task to automakers for the purpose of fuel efficiency and emission control without sacrificing the vehicle safety. One of the remarkable attempts is the ULSAB-AVC(Ultra Light Steel Auto Body - Advanced Vehicle Concepts) project which has been carried out under the International Iron and Steel Institute(IISI) for light-weight design and increase of fuel efficiency by substituting the advance high strength steel(AHSS) for the conventional low strength steel and applying the recent forming technique such as hydro-forming and tailor-welded blank so as to reduce the number of parts and guarantee the strength of each part.

The strict regulation for the side impact test has been legislated and executed to assure of passenger safety. Automotive companies must satisfy the safety regulation of each country in order to export cars to the country and obtain higher star-rating to prevail in competition with other automotive companies. For the purposes, optimum design of each part has been carried out and new forming techniques are applied to main parts of an auto-body. In addition, the advance high strength steel is applied to important parts to achieve the light-weight design and improve the crashworthiness of an auto-body.

In this paper, the side impact analysis of the ULSAB-AVC model with the conventional steel (ULSAB-AVC-CS model) and the AHSS (ULSAB-AVC-AHSS model) is performed to compare the crashworthiness between the two models. The analysis evaluates the deformed shape, the intrusion velocity and the distance pushing into the cabin room quantitatively to investigate the effect of the AHSS on the crashworthiness.

2. Side Impact Regulation

One of the important regulations for the side impact test is US-SINCAP(U.S. Side Impact test for New Car Assessment Program) based on the FMVSS 214D of the NHTSA under the U.S. department of transportation. This test uses a regulated moving deformable barrier (MDB) to strike a side of a test vehicle at the angle of 27° with the initial velocity of 61.96kph(38.5mph) as shown in Figure 1. The face of a barrier is made of an aluminum honeycomb block and an aluminum bumper. The bottom of the edge of the MDB is located at the height of 279mm from the ground. The protruding length of the barrier is 102mm and the total depth of the MDB is 483mm to the moving direction. The total weight of the MDB is 1,361kg and the regulated impact
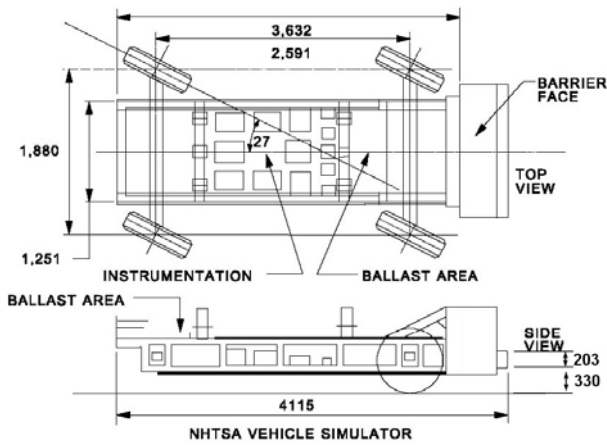
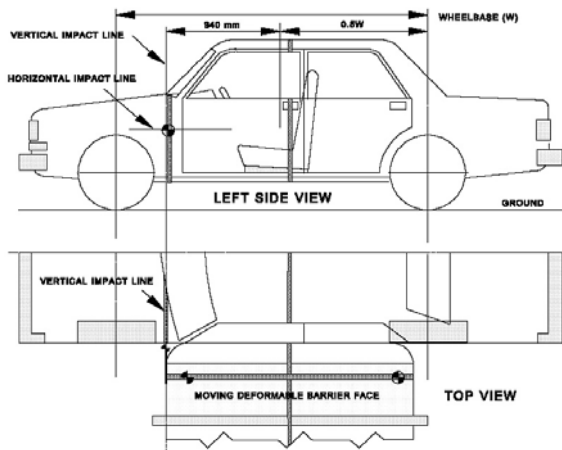Figure 1. Moving deformable barrier for the SINCAP test

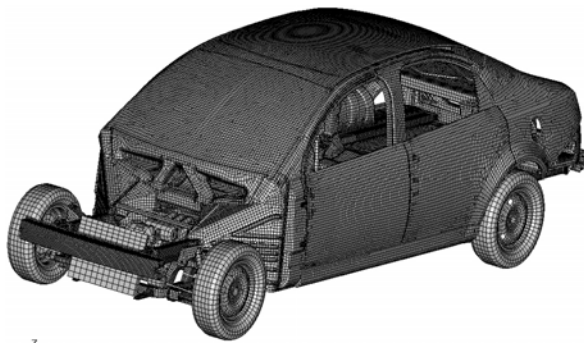Figure 2. Schematic diagram of impact line for SINCAP test procedure

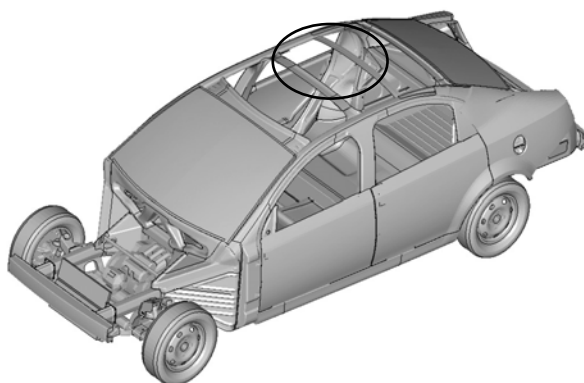Figure 3. Finite Element model for the side impact analysis of ULSAB-AVC vehicle


Figure 4. Roof crossmember

line is aligned as shown in Figure 2 when the MDB bumps against the test vehicle. Since the length of the wheelbase of the ULSAB-AVC model(PNGV-Class) is larger than 2,896mm for the impact test, the impact line must be placed on 508mm ± 5mm rearward of the test vehicle's front axle. The total weight of a test vehicle is calculated by summing up the unloaded vehicle weight (UVW), the rated capacity luggage weight (RCLW) and two side impact dummies (SID). To satisfy this mass condition, mass elements are distributed on the whole area of an auto-body. Two SIDs are seated in the driving seat and the back of driving seat. The injury level for evaluation of a developed auto-body is calculated from sensors that are placed on the part of pelvis, spine and rib of a SID.
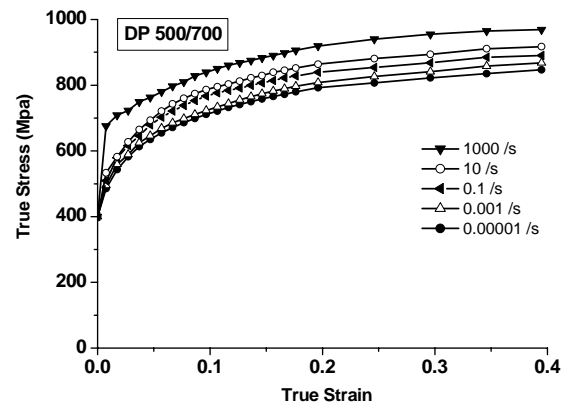
(a)
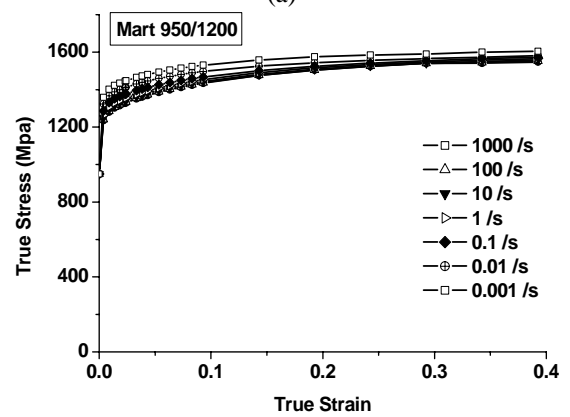
(b)
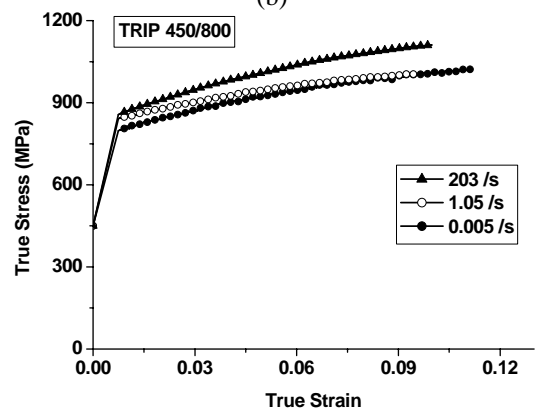
(c)

Figure 5. Dynamic stress-strain curves of the AHSS with various strain rate: (a) DP400/700; (b) Mart950/1200; (c) TRIP 450/800

Table 1 Mechanical properties used in ULSAB-AVC-AHSS model[7]

Steel Grade	YS (MPa)	UTS (MPa)	Total EL (%)	n-value (5-15%)	r-bar	K-value (MPa)
BH 210/340	210	340	34-39	0.18	1.8	582
BH 260/370	260	370	29-34	0.13	1.6	550
DP 280/600	280	600	30-34	0.21	1.0	1082
IF 300/420	300	420	29-36	0.20	1.6	759
DP 300/500	300	500	30-34	0.16	1.0	762
HSLA 350/450	350	450	23-27	0.14	1.1	807
DP 350/600	350	600	24-30	0.14	1.0	976
DP 400/700	400	700	19-25	0.14	1.0	1028
TRIP 450/800	450	800	26-32	0.24	0.9	1690
DP 500/800	500	800	14-20	0.14	1.0	1303
CP 700/800	700	800	10-15	0.13	1.0	1380
DP 700/1000	700	1000	12-17	0.09	0.9	1521
Mart 950/1200	950	1200	5-7	0.07	0.9	1678
Mart 1250/1520	1250	1520	4-6	0.065	0.9	2021

Table 2 Mechanical properties used in ULSAB-AVC-CS model

	Thickness (mm)	Yield Stress (MPa)	Ultimate Stress (MPa)	Strain (at Ult Stress)	Elongation	K	ε_p	n
SPCD	0.7	149.14	298.78	0.296	0.588	560.53	0.00811	0.275
SPCUD	0.7	135.39	288.49	0.282	0.607	549.02	0.00723	0.284
SGACD	0.79	165.62	307.94	0.256	0.567	560.3	0.0084	0.255
SPCEN	0.7	148.50	295.13	0.282	0.607	556.19	0.00895	0.28
SPRC340S	0.81	213.14	349.7	0.230	0.487	638.89	0.0135	0.255
SPRC35R	0.7	199.61	345.17	0.252	0.497	625.62	0.0111	0.254
SPRC35E	0.7	198.55	369.51	0.253	0.477	687.09	0.0094	0.266
SPCC	0.79	270.56	356.51	0.246	0.482	641.32	0.033	0.253
SPRC390-BH	0.65	268.0	399.53	0.211	0.43	696.94	0.0154	0.229
SPRC40R	1.0	316.02	425.18	0.213	0.465	726.88	0.0193	0.211
SPRC45E	1.19	312.08	464.99	0.211	0.458	832.13	0.0168	0.24
SPFC590	1.21	435.79	648.75	0.218	0.37	1177.0	0.0197	0.253
TRIP 60	1.21	423.82	645.63	0.226	0.372	1161.55	0.0166	0.246
SPFH590	3.05	553.04	644.18	0.130	0.285	974.46	0.018	0.141
SPFC780	1.19	523.42	842.66	0.137	0.24	1319.83	0.0021	0.15
TRIP 80	1.2	563.22	859.68	0.144	0.23	1440.39	0.00642	0.186
SPFC980	1.19	693.44	1064.63	0.0894	0.175	1545.9	0.00073	0.111

3. Side Impact Model

The side impact analysis is carried out with a finite element model based on the ULSAB-AVC model. The finite element model is constructed with 205,000 shell, solid and beam elements as shown in Figure 3. The side impact analysis is performed with a modified ULSAB-AVC model in which two roof crossmembers are added as reinforcement to enhance the crashworthiness and stabilize the analysis as described in Figure 4. The analysis was performed with the use of a finite element explicit code, LS-DYNA3D v.970, with the piecewise-linear material model considering the elasto-plastic material nonlinearity. The analysis considers the effect of the strain rate with the dynamic material properties of auto-body steels obtained by experiments at various strain rates. Figure 5 shows the stress-strain curves of the AHSS with respect to the strain rate. The ULSAB-AVC model is made up of the advance high strength steel for about 85% of the body as shown in Table 1. For the sake of simplicity of the side impact analysis, the two SIDs are removed in calculation of the injury level. Instead, two lumped masses having 76.5kg are applied on the center of each seat crossmember.

4. Side Impact Analysis

The crashworthiness in the side impact is evaluated with the ULSAB-AVC-AHSS and the ULSAB-AVC-CS model. The AHSS is replaced by the conventional steel to compare the crashworthiness of the two crash models. The material properties of conventional steels are acquired at various strain rates to consider the stain rate hardening effect. Table 2 shows the list of the conventional steels applied in the ULSAB-AVC-CS model. And the representative stress-strain curves are plotted in Figure 6. The side impact analysis is performed during the crashing time of 60msec. The Figure 7 shows comparison in the deformed shapes between the ULSAB-AVC-AHSS and the ULSAB-AVC-CS after collision. Amount of the total deformation increases remarkably when conventional steels are adopted. The B-pillar connected to the floor and the roof also deforms severely compared to the ULSAB-AVC-AHSS model. The deformation along the cross section of a test vehicle is investigated to compare the deformed shapes closely as shown in Figure 8(a) and 9. The roof and floor region are severely collapsed after the side impact test. Amount of energy absorption is demonstrated for each member in Figure 10 during the side impact test. The members which have an important role in the energy absorption are the
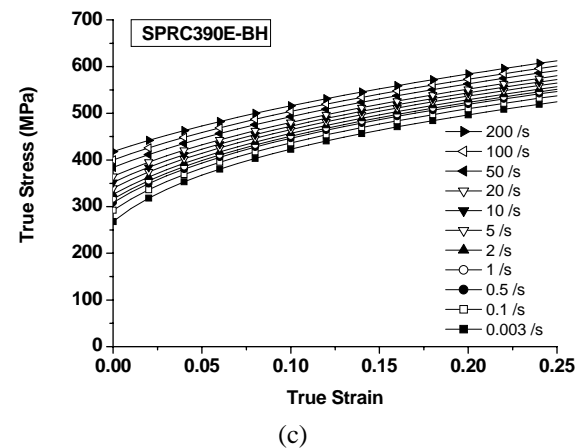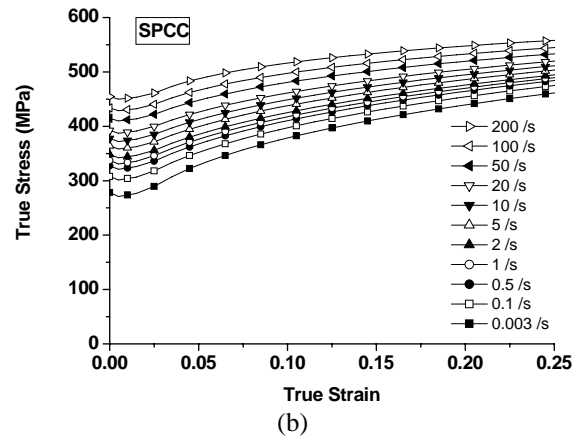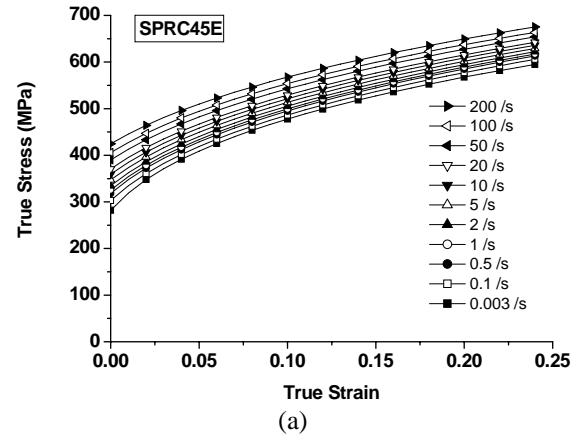

Figure 6. Dynamic stress-strain curves of the conventional low strength steels with various strain rate: (a) SPRC45E; (b) SPCC; (c) SPRC390E-BH

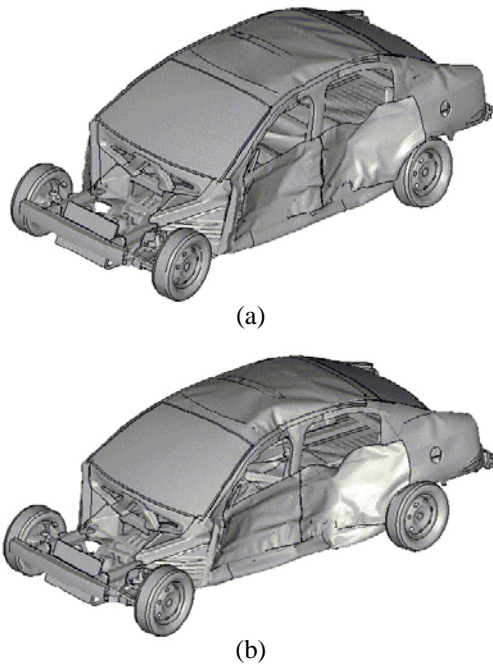(a)

(b)

Figure 7. Deformed shapes of the vehicle for the crash analysis at time 0.06sec: (a) ULSAB-AVC-AHSS model; (b) ULSAB-AVC-CS model
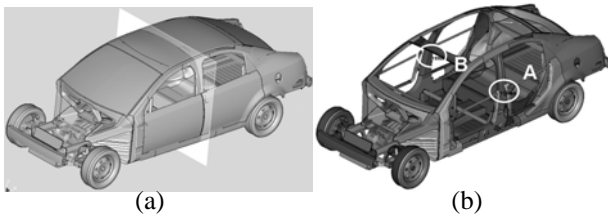

(a)   (b)

Figure 8. Geometric information for the measurement of deformation amount, the intrusion displacement and the intrusion velocity: (a) cross section; (b) measuring point A and B
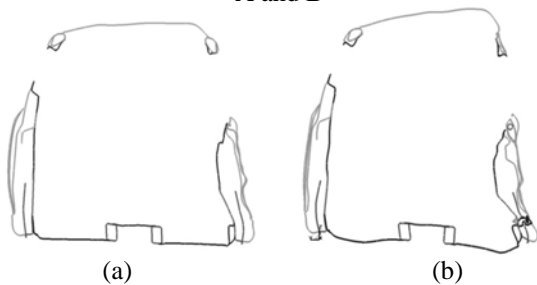

(a)   (b)

Figure 9. Deformed shapes of the cross section at final collision : (a) ULSAB-AVC-AHSS model; (b) ULSAB-AVC-CS model
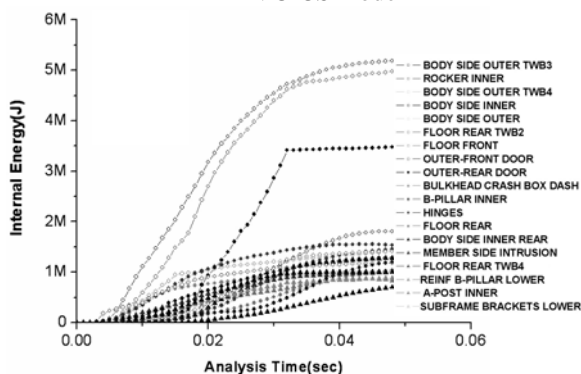

Figure 10. Energy absorption characteristics of important members during the side impact test

bodyside outer panel, the rocker inner member, the bodyside inner panel and the floor rear. Figure 11 shows the position and the shape of the energy absorption parts. The reinforcement of the B-pillar inner is bent and intruded to a cabin room since it can not sustain the external load. The intrusion distance of the ULSAB-AVC-CS model increases as large as twice of that of the ULSAB-AVC-AHSS model. These results explain that the crashworthiness of the ULSAB-AVC-CS model is incomparably worse than the ULSAB-AVC-AHSS model. The ULSAB-AVC-CS model can not guarantee the affordable cabin room and acceptable injury level during the impact test. The intrusion velocity and the distance between A and B in Figure 8(b) are compared to each other. The point A is placed on the inner panel (2306mm, -700mm, 756mm) and B is placed on the other side inner panel of the B-pillar (2306mm, -700mm, 756mm) from the reference point as depicted in Figure 12. The intrusion distance of an auto-body is calculated by subtracting two intruded displacements on the position A and B to remove the rigid body motion. The intrusion distance is 133mm in the ULSAB-AVC-AHSS model. On the other side, the intrusion distance in the ULSAB-AVC-CS model increases to 282.5mm more than twice of that in ULSAB-AVC-AHSS model as depicted in Figure 13. The initial peak of the intrusion velocity and the maximum intrusion velocity of the ULSAB-AVC-CS model are much higher than those of the ULSAB-AVC-AHSS model as shown in Figure 14.The intrusion velocity of the ULSAB-AVC-CS model increases continuously and becomes larger than the initial peak while the intrusion velocity of the ULSAB-AVC-AHSS model does not reach the maximum initial peak again after the initial peak is occurred. In order to investigate these procedures, the five important points are designated for observation as shown in Figure 15(a) and (b). The initial peak of the intrusion velocity occurs at the instance when the MDB bumps against the test car and a door panel starts to collapse. The intrusion velocity, then, decreases when the door panel is totally collapsed and the B-pillar sustains the external load. The intrusion velocity increases again when the outer panel of the B-pillar can not support the external load. The outer panel of the B-pillar having the initial curvature starts to collapse to the opposite direction.
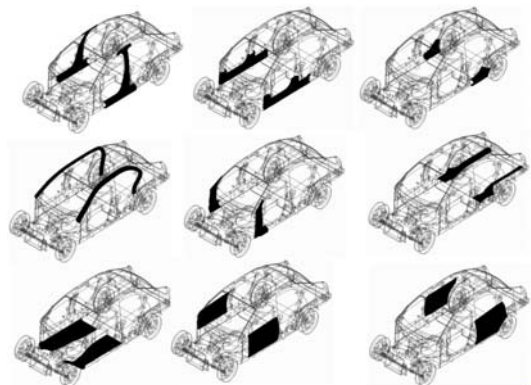

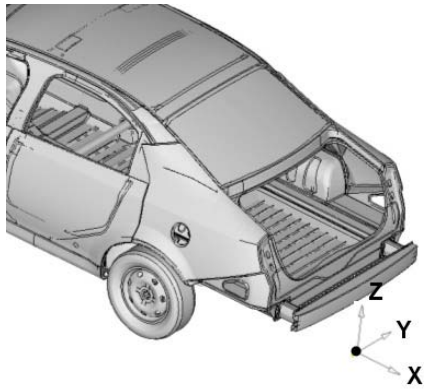Figure 11. Critical members for energy absorption
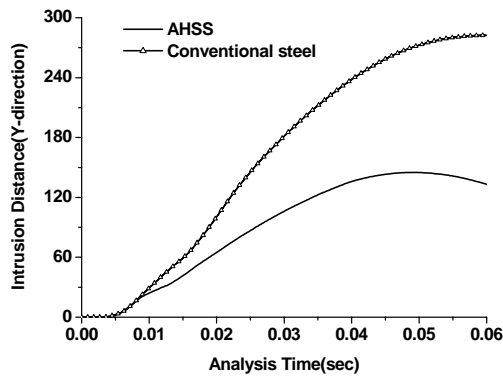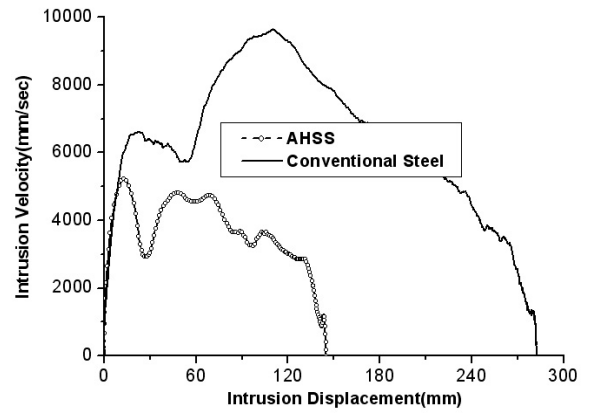
Figure 12. Reference point

Figure 14. Variation of intrusion velocity of a B-pillar with respect to the time: (a) ULSAB-AVC-AHSS model; (b) ULSAB-AVC-CS model

Figure 13. Amount of intrusion distance of a B-pillar with respect to analysis time
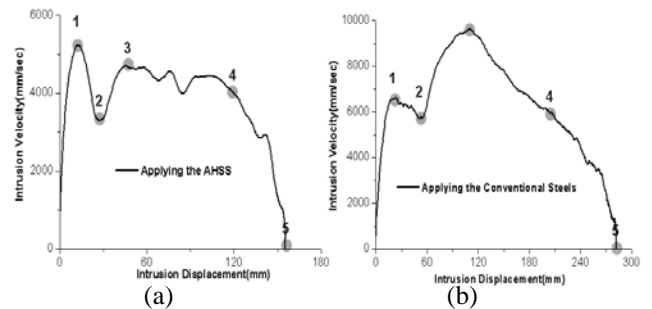

(a)   (b)

Figure 15. Points of time at which the local minimum and local maximum velocity occurs: (a) AHSS; (b) conventional Steel
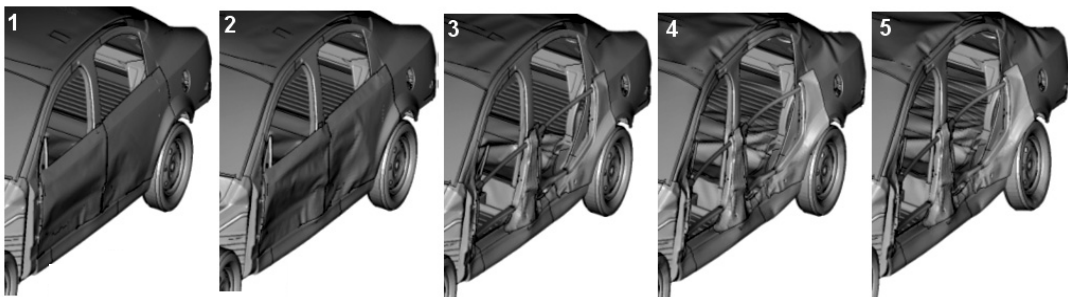

Figure 16. Subsequent deformation mechanism with AHSS: (1) 0.007sec; (2) 0.011 sec; (3) 0.016 sec; (4) 0.03 sec; (5) 0.047 sec
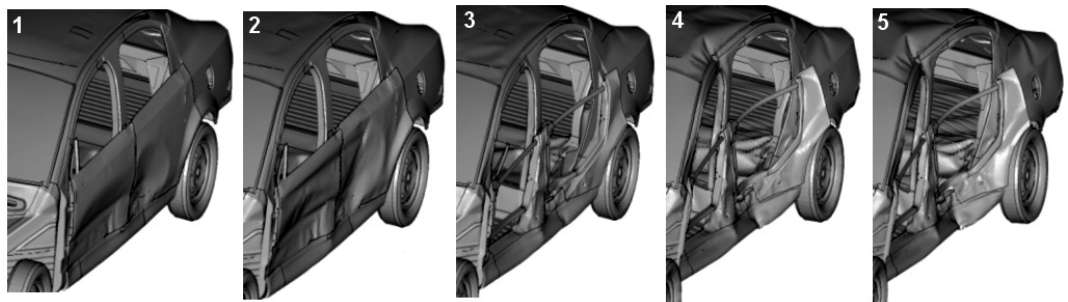

Figure 17. Subsequent deformation mechanism with conventional low strength steel: (1) 0.0088sec; (2) 0.0143 sec; (3) 0.02 sec; (4) 0.04 sec; (5) 0.06 sec

However, the intrusion velocity of the ULSAB-AVC-AHSS model does not reach the initial peak again because the roof and the B-pillar does not collapse and maintains the original shape as depicted in Figure 16(5). The intrusion velocity of the point A and B comes to decrease after this procedure, and then an auto-body experiences the rigid body motion and moves together since the intrusion velocity becomes zero after the instance 5.

4. Conclusion

This paper investigated the effect of the AHSS on the crashworthiness in the side impact case under the regulation of US-SINCAP. The ULSAB-AVC model is utilized to analyze the crashworthiness with the adoption of the advance high strength steel and the conventional low strength steel. The most parts of ULSAB-AVC model with the AHSS are replaced by the conventional low strength steels. The analysis of the side impact test is carried out with the material properties obtained with the variation of the strain rate for strain rate hardening. The intrusion velocity and distance of the ULSAB-AVC-AHSS model decrease tremendously compared to the ULSAB-AVC-CS model. The results demonstrate that an auto-body with the AHSS maintains affordable cabin room and guarantees to decrease passenger's injury level during the side impact. The crashworthiness with the ULSAB-AVC-AHSS model is improved almost twice of that with the ULSAB-AVC-CS model.

4. References

[1] H. Huh, J. H. Lim, J. H. Song, K. S. Lee, Y. W. Lee and S. S. Han, "Crashworthiness Assessment of Side Impact of an Auto-Body with 60TRIP Steel for Side Members", International Journal of Automotive Technology, Vol. 4, No. 3, pp.149-156, 2003

[2] H. Huh, J. H. Lim, S. B. Kim, S. S. Han, S. H. Park, "Formability of the Steel Sheet at the Intermediate Strain Rate", Key Engineering Materials, Vol. 274-276, pp.403-408, 2004

[3] J. Cafolla, R. W. Hall, D. P. Norman, "Forming to Crash Simulation in Full Vehicle Models", 4th European LS-DYNA Users Conference, Metal Forming II, E-II-17-26, 2003

[4] S. Simunovic, J. Shaw, G. A. Aramayo, "Steel Processing Effects on Impact Deformation of Ultra Light Steel Auto Body" , SAE Paper, 2001-01-1056, 2001

[5] H. Huh, K. P. Kim, S. H. Kim, J. H. Song, H. S. Kim and S. K. Hong, "Crashworthiness Assessment of Front Side Members in an Auto-Body Considering the Fabrication Histories", Int. J. Mech. Sci., Vol. 45, pp. 1645-1660, 2003

[6] ULSAB-AVC Program Technical Transfer Dispatch#1-6, Porsche Engineering Services, Inc., 1999

[7] ULSAB-AVC Engineering Report, Porsche Engineering Services, 2001

[8] LSTC, LS-DYNA970 Keyword User's Manual, Livermore, 2003